USITP-10/96
UUITP-1/97
CU-TP-810
CAL-627
astro-ph/9702037

Astrophysical-Neutrino Detection with Angular and Energy Resolution

Lars Bergström*
Department of Physics, Stockholm University, Box 6730, SE-113 85 Stockholm, Sweden

Joakim Edsjö†
Department of Theoretical Physics, Uppsala University, Box 803, SE-751 08 Uppsala, Sweden

Marc Kamionkowski‡
Department of Physics, Columbia University, 538 West 120th Street, New York, New York 10027, U.S.A.

(February 4, 1997)

Abstract

We investigate the improvement in sensitivity to astrophysical point sources of energetic ($\gtrsim 1$ GeV) neutrinos which can be achieved with angular and/or energy resolution of the neutrino-induced muon. As a specific example we consider WIMP annihilation in the Sun and in the Earth as a neutrino source. The sensitivity is improved by using the angular and energy distribution to reduce the atmospheric-neutrino background. Although the specific improvements depend on the backgrounds and assumed sources, the sensitivity to a WIMP signal may be improved, with equal exposure, by up to roughly a factor of two with good angular resolution, and by up to roughly a factor of three with good energy resolution. In case of a positive detection, energy resolution

*E-mail address: lbe@physto.se

†E-mail address: edsjo@teorfys.uu.se

‡E-mail address: kamion@phys.columbia.edu

would also improve the measurement of the neutrino energy spectrum and therefore provide information on the WIMP mass and composition.

I. INTRODUCTION

High-energy neutrino astrophysics is a rapidly growing field at the interface of particle physics and astrophysics. In addition to the high-energy neutrinos expected from various cosmic accelerators, neutrinos with energies in the range of $\mathcal{O}(1-1000\,\mathrm{GeV})$ may be produced by the annihilation of weakly-interacting massive particles (WIMPs) at the core of the Sun and/or Earth if WIMPs populate the Galactic halo [1,2]. Detection of such neutrinos would be revolutionary for cosmology and for particle physics.

Several detectors capable of detecting such neutrinos, such as Baksan [3], IMB [4], Kamiokande II [5], MACRO [6], and Frejus [7] have already put important constraints on the fluxes of such neutrinos, and the sensitivity should increase dramatically with the advent of several new experiments such as Super-Kamiokande [8], AMANDA [9], NESTOR [10], and perhaps others [11].

Given a specific WIMP candidate—for example, a neutralino in a supersymmetric extension of the standard model—calculation of the differential energy spectrum of the neutrino is straightforward [12,13]. Neutrinos are produced by decays of the WIMP annihilation products, so the detailed energy spectrum depends on the mass of the neutralino and on its composition. The mean neutrino energy generally rises with increasing WIMP mass.

A high-energy neutrino is inferred through observation of an upward muon produced by a charged-current interaction of the neutrino in the rock (or ice) below the detector. (Downward muons can similarly be produced, but these rare events are usually overwhelmed by the enormous flux of downward muons from cosmic-ray showers in the atmosphere.) Given a point source of neutrinos with some energy distribution, muons are produced with a distribution of energies and angles. The mean muon energy increases with the mean neutrino energy, and the average angle of production decreases with increasing neutrino energy. Unfortunately, although these detectors have decent angular resolution, they have little or no energy resolution. The muon range in matter is roughly proportional to its production energy. Since we cannot tell where the muon was produced, we cannot determine its energy. All we can say is that if it passes through the entire detector, it must have an energy greater than some threshold E_{thresh} which, for example, is roughly 2 GeV for IMB, Kamiokande II, and MACRO.

Since the cross section for muon production is proportional to the energy as is the mean muon range, the probability of detecting a neutrino depends on the square of the neutrino energy. Although each WIMP candidate may produce a different neutrino energy distribution, the flux of neutrino-induced muons depends only on the second moment of the neutrino energy spectrum.

If there were no backgrounds, one could simply look for neutrinos by looking for upward muons from the point source of interest. Of course, due to the finite muon production angle, we would want to accept muons from a large enough solid angle around the point source to assure that we were getting all the events. For example, the rms angle between the neutrino direction and the direction of the induced muon is $\sim 20^\circ (E_\nu/10\,\mathrm{GeV})^{-1/2}$. Furthermore, the muon typically carries half the neutrino energy, so the angular radius of the acceptance cone should be $\sim 14^\circ (E_\mu/10\,\mathrm{GeV})^{-1/2}$. A null result after some exposure would then translate into an upper limit to the second moment of the neutrino energy spectrum and thus constrain WIMP candidates.

However, neutrino point sources must be distinguished from a background of atmospheric neutrinos with an energy spectrum which falls roughly as a power law. The atmospheric-neutrino background is nearly isotropic (on small enough angular scales), so the flux is proportional to the solid angle of the acceptance cone around the point source. If only the second moment (and no further information) of the WIMP neutrino energy distribution is specified, the background flux is that in a cone large enough to include all muons which may have been produced by a neutrino with energy just large enough to produce a muon above threshold. This produces a conservatively large estimate of the background and thus a conservative sensitivity to the point source of interest. Improving the sensitivity in this single-bin approach by optimizing the angular cut has been studied in Ref. [14] and we will compare with that approach later.

Models for candidate point sources of astrophysical neutrinos (such as the example of WIMP annihilation in the Sun and Earth on which we focus here) predict the energy distribution of the neutrinos, and therefore the muon angular and energy distribution can also be predicted. These differ from the angular and energy distribution of the atmospheric-neutrino background, so experimental determination of the muon energies and directions can be used to discriminate between sources and backgrounds.

In this paper we quantify the improvements to the sensitivity of astrophysical neutrino point sources that can be achieved if the direction and energy of the neutrino-induced muon can be resolved. If the direction of the muons can be measured with higher resolution than the width of the angular distribution of the signal, the signal-to-noise ratio can be increased with the same exposure. This is analogous to the use of the nuclear recoil-energy distribution in direct-detection experiments [15]. We also calculate the further improvement in the sensitivity if the experiment has energy resolution as well.

We estimate the sensitivity to a signal in several ways. We will assume that the background flux is known (we also compare with the case of it being unknown) and consider the sensitivity to a signal given either that it comes from a general WIMP or that it comes from a WIMP with a specific mass and composition. We find that angular resolution can improve the sensitivity, for fixed exposure, roughly by a factor of 2 (depending on backgrounds and signal fluxes), and that the sensitivity can be improved by up to roughly a factor of 3 if there is both angular and energy resolution.

In the following Section, we describe how we calculate the expected sensitivities, and in Section III we present numerical results for some representative models. We then close with some concluding remarks in Section IV and present a table of numerical results in an Appendix.

II. CALCULATIONAL METHOD

A. Introduction

Consider a theory which predicts an upward-muon flux ϕ_s (where the s stands for "signal") with an angular distribution $d\phi_s/d\theta = \phi_s^0 f_s(\theta) \sin\theta$, where θ is the angle the muon makes with the direction of the point source of interest, and $\int f_s(\theta) \sin\theta \, d\theta = 1$ (i.e., $f(\theta)$ is constant for an isotropic distribution). We would like to disentangle this signal from

a background of atmospheric neutrinos which has a flux ϕ_b with an angular distribution $d\phi_b/d\theta = \phi_b^0 f_b(\theta)\sin\theta$, which is nearly isotropic (at least on small angular scales).

Consider first an experiment that can only tell that a muon has been detected with an angle $\theta \leq \theta_{\rm max}$, but no further information on the muon direction is available. Alternatively, suppose an experiment can only detect muons above some energy threshold $E_{\rm thresh}$ with no further information on the energy. If we wish to derive an upper limit to the neutrino flux from a point source in a model-independent fashion, we must make the most conservative assumption that all the muon energies were near threshold. Then, the angular acceptance cone around the source must be large enough to include all (or most) of the muons produced by neutrinos from the point source. One would therefore have some number of muons detected with an angle $\theta \leq \theta_{\rm max}$. For example, in their searches for energetic neutrinos from the Earth and Sun, the Baksan collaboration [3] reports the flux of muons within an angle $\theta_{\rm max} = 30^\circ$ of the Sun or the center of the Earth. The Kamiokande collaboration [5] reports the flux of muons within an angle varying between $\theta_{\rm max} = 5^\circ$–$30^\circ$.

With such a result, the number of background events after an exposure $\mathcal{E}$ (for example, in units of km^2 yr) is $N_b = \mathcal{E}\phi_b^0 \int_0^{\theta_{\rm max}} f_b(\theta)\sin\theta\, d\theta$. The number of expected events from the source of interest is $N_s = \mathcal{E}\phi_s^0 \int_0^{\theta_{\rm max}} f_s(\theta)\sin\theta\, d\theta \simeq \mathcal{E}\phi_s^0$, where we have made the reasonable assumption that signal muons come from the vicinity of $\theta = 0$. A 3σ detection would require an excess of $3\sqrt{N_b + N_s}$ events over the number expected. Then, a 3σ excess will be observable only if $\phi_s > 3\sigma$ where $\sigma = \sqrt{N_b + N_s}/\mathcal{E}$. For an isotropic background, $f_b(\theta) = 1/2$, so $\sigma \simeq [(1 - \cos\theta_{\rm max})\phi_b/(2\mathcal{E})]^{1/2}$. Thus, the sensitivity scales as the inverse square root of the exposure. Furthermore, since $\theta_{\rm max}$ scales as $E_{\rm thresh}^{-1/2}$, the sensitivity of the experiment improves as $E_{\rm thresh}^{-1/2}$, assuming the energies of most signal muons are above threshold and $\theta_{\rm max} \ll 1$.

From such a simple experiment described above where no energy or angular distributions are used, we can conclude that the minimal exposure required for a 3σ discovery is

$$\mathcal{E}_{\rm min} = \frac{9\,(\phi_b + \phi_s)}{\phi_s^2} \tag{1}$$

where ϕ_b and ϕ_s are the background and signal fluxes above threshold and within the angular cone of acceptance $\theta_{\rm max}$. Note that Eq. (1) is only valid when the fluxes are high. This minimal exposure is relevant to the way, e.g., Baksan and Kamiokande have analyzed their data (with different values of $\theta_{\rm max}$). In the following more detailed examples, Eq. (1) with $\theta_{\rm max} = 5^\circ$ will be used for comparison. Note that for low masses ($\lesssim 100$ GeV) the optimal $\theta_{\rm max}$ will be higher and for high masses it will be lower. However, one cannot know in advance what the optimal cut will be. Hence we have chosen 5° as a reasonable compromise giving decent results both for low and high masses.

B. Covariance-Matrix Analysis

Now consider a slightly more sophisticated experiment which has angular and/or energy resolution. It is possible that we will actually be fitting for both a background and a signal flux of muons where the background flux is given by

$$\frac{d^2\phi_b}{dEd\theta}(E,\theta) = \phi_b^0 f_b(E,\theta), \tag{2}$$

which we assume to be isotropic (at least over small angular patches), $f_b(E,\theta) = f_b(E)$. We will only consider the atmospheric background resulting from cosmic-ray interactions in the Earth's atmosphere. This is an irreducible background that cannot be avoided even in very deep underground detectors. In addition, we will want to fit data for an annihilation signal which generally depends on the WIMP mass m_χ and on the WIMP composition. We may parameterize this as

$$\frac{d^2\phi_s}{dEd\theta}(E,\theta) = \phi_s^0 \left[a f_{\rm hard}(m_\chi, E, \theta) + (1-a) f_{\rm soft}(m_\chi, E, \theta)\right], \tag{3}$$

where a parameterizes the relative contributions of a "hard" and "soft" annihilation spectrum. As a "hard" annihilation spectrum we have used the $\tau^+\tau^-$ channel below the W-mass and W^+W^- above and as a soft spectrum we have used $b\bar{b}$. These channels represent the extreme hardnesses of the spectrum for any given WIMP mass. For the evaluation of the neutrino and muon flux for these channels we have used the method given in Ref. [13], where the whole chain of processes from the annihilation products in the core of the Sun or the Earth to detectable muons at the Earth was considered.

Therefore, we are assuming that the muon angular and/or energy distribution from both background and signal will be described by the set of parameters, $\mathbf{s} = \{\phi_b^0, \phi_s^0, m_\chi, a\}$ (one could also envision more parameters). We now want to ask, with what precision can we measure these parameters with a given experiment, assuming the true distribution is given by some set of parameters, $\mathbf{s}_0$?

To do so, we assume the data is binned into a number of angle/energy bins, and each bin i is centered on angle θ_i and energy E_i with widths ΔE_i and $\Delta\theta_i$. Therefore, for a given set $\mathbf{s}$ of parameters, the flux will be

$$\frac{d^2\phi}{dEd\theta}(E,\theta;\mathbf{s}) = \frac{d^2\phi_b}{dEd\theta}(E,\theta;\mathbf{s}) + \frac{d^2\phi_s}{dEd\theta}(E,\theta;\mathbf{s}), \tag{4}$$

where we have written the dependence of the flux on the model parameters $\mathbf{s}$. The probability distribution for the number of events expected in each bin is a Poisson distribution with mean $N_i = \mathcal{E}\frac{d^2\phi}{dEd\theta}(E_i,\theta_i)\Delta E_i \Delta\theta_i$, so it has a width $\sigma_i = \sqrt{N_i}$.

So, suppose the true parameters are $\mathbf{s}_0$. Then the probability distribution for observing an angle/energy distribution which is best fit by the parameters $\mathbf{s}$ is

$$P(\mathbf{s}) \propto \exp\left[-\frac{1}{2}(\mathbf{s}-\mathbf{s}_0)\cdot[\alpha]\cdot(\mathbf{s}-\mathbf{s}_0)\right], \tag{5}$$

where the curvature matrix $[\alpha]$ is given approximately by

$$\begin{aligned}\alpha_{ab} &= \mathcal{E}\sum_i \frac{1}{\sigma_i^2}\frac{\partial N_i}{\partial s_a}\frac{\partial N_i}{\partial s_b} \\ &= 4\mathcal{E}\sum_i \frac{\partial\sqrt{N_i}}{\partial s_a}(\mathbf{s}_0)\frac{\partial\sqrt{N_i}}{\partial s_b}(\mathbf{s}_0),\end{aligned} \tag{6}$$

where the partial derivatives are evaluated at $\mathbf{s} = \mathbf{s}_0$, and we used $\sigma_i = \sqrt{N_i}$ in the second line. In a realistic experiment, the width of the bins would be comparable to the angular and/or energy resolution of the experiment. In the limit of perfect angular and energy resolution, the sum becomes an integral,

$$\alpha_{ab} = 4\mathcal{E} \int\int dE\, d\theta\, \frac{\partial\sqrt{d^2\phi(E,\theta;\mathbf{s})/dEd\theta}}{\partial s_a}\, \frac{\partial\sqrt{d^2\phi(E,\theta;\mathbf{s})/dEd\theta}}{\partial s_b}. \tag{7}$$

The covariance matrix, $[\mathcal{C}] = [\alpha]^{-1}$ gives an estimate of the standard errors that would be obtained from a maximum-likelihood fit to data: The standard error in measuring the parameter s_a (after marginalizing over all the other undetermined parameters) is approximately $\sigma_a \simeq \mathcal{C}_{aa}^{1/2}$. If three times the standard error in ϕ_s^0 is less than ϕ_s^0, for a given underlying model $\mathbf{s}_0$ and for a given experiment, then this model will be distinguishable from background at the 3σ level.

If all of the parameters except for ϕ_s^0 are fixed, then $[\alpha]$ is a 1×1 matrix, i.e., $1/\sigma^2$. In this case, Eq. (7) reduces to

$$\frac{1}{\sigma^2} = \mathcal{E} \int\int \frac{[f_s(\theta,E)]^2}{\phi_b^0 f_b(E) + \phi_s^0 f_s(\theta,E)} \sin\theta\, d\theta\, dE. \tag{8}$$

To illustrate, if there were no background, Eq. (8) says that the statistical uncertainty in the number of events is the square root of the number of events, and this makes sense. However, if the total number of events is nonzero, then a signal has been discovered. In other words, a 99% CL does not correspond to 3σ for small numbers.

In fact, if there is no background, and an event is seen, it constitutes discovery. On the other hand, if nothing is seen, the 95% CL upper limit to the number is 3.

III. RESULTS

We are now ready to perform some actual calculations using the techniques described in the previous Section for the specific example of WIMP annihilation in the Sun and Earth. WIMPs which are gravitationally trapped in the Sun/Earth can annihilate to produce neutrinos which reach a neutrino telescope, interact, and form detectable muons. For the muon fluxes we have used the method given in Ref. [13] where all relevant processes from the WIMP annihilation products to the resulting muon flux at a detector are calculated using Monte Carlo simulations. The muon fluxes are calculated for different WIMP masses and annihilation channels. We assume that the neutrino energy spectra are either the hard or soft spectra described above; energy spectra from realistic WIMP candidates should fall somewhere between these two extremes. Since the muon flux is proportional to the neutrino energy squared, the hard annihilation channels will generally be more important and hence in general the muon spectra will be more hard than soft. Because of the steep fall with energy of the atmospheric background, hard spectra generally require less exposure. In all integrations with angular (and energy) distribution the integration in Eq. (7) is performed up to $\theta = 30^\circ$. For the atmospheric background we have used the results given in Ref. [16].

Even though the absolute value of the background flux is uncertain by some 20%, the overall level will certainly be measured with high accuracy by the new experiments.

In Tables I–III in the Appendix, the minimal exposures required for a 3σ discovery are given for detectors with no angular resolution, only angular resolution and angular and energy resolution assuming that all four parameters in Eq. (3) are unknown, only the three signal parameters are unknown and only ϕ_s^0 is unknown. In Figs. 1–3 some illustrative examples of these results are shown and in the following subsections these results are described and discussed.

A. Detector with angular resolution

If we assume that the background flux is known (by, e.g., an off-source measurement) and that all three parameters in Eq. (3) corresponding to the signal flux are unknown we need at least the exposures given in Fig. 1 to be able to make a 3σ discovery if we have perfect angular resolution but no energy resolution.

Note that the spread between soft and hard spectra is due to our ignorance of the actual branching ratios into different annihilation channels and the two curves for soft and hard should thus be treated as extreme values. However, as explained earlier, in general spectra will be closer to being hard than being soft. We also see that when the signal flux is high, the difference between soft and hard spectra does not matter since in this case the signal-to-noise ratio is high even though the spectra are smeared.

By comparing Figs. 1(a) and (b), we see that the exposures needed when looking at the Sun horizontally are about a factor of 2 higher when the signal flux is low due to the atmospheric background being higher in the horizontal direction than in the vertical. When the signal flux is high, the needed exposures are about the same.

If we compare Figs. 1(a) and (b) with (c), we find that the curves for the Earth are more dependent on the mass than the curves for the Sun, being higher at low masses and lower at high masses. At low masses this difference is because the size of the annihilation region is non-negligible in the Earth and is thus making the angular distributions wider. For high masses the difference is due to the fact that neutrino interactions on the way out of the Earth are negligible while they are not for the Sun thus softening the Sun spectra at high masses.

So far we have considered a detector with perfect angular resolution. In Fig. 2 we show an example of what happens if we add experimental angular resolution. As expected the needed exposures are higher at high masses since we now cannot make use of the highly collimated signal flux at these high masses. The general trend for other fluxes and for the Sun is the same as that shown in the Figure. In the Figure, curves for different energy thresholds are also given. These are described in next subsection.

In Fig. 3 we evaluate the sensitivities attainable if we marginalize over m_χ and a ("3 par") and if we marginalize over ϕ_b^0 as well ("4 par"). To compare, we also show the sensitivities assuming these parameters are fixed and we are just fitting for the source flux ϕ_s^0 ("1 par"). We also compare with the case of just using one bin up to $\theta_{\max} = 5^\circ$ and checking if any signal above background can be seen in this single bin. We see that we gain a factor of 2–3 by knowing the background flux in advance (which is quite reasonable). Note that the position

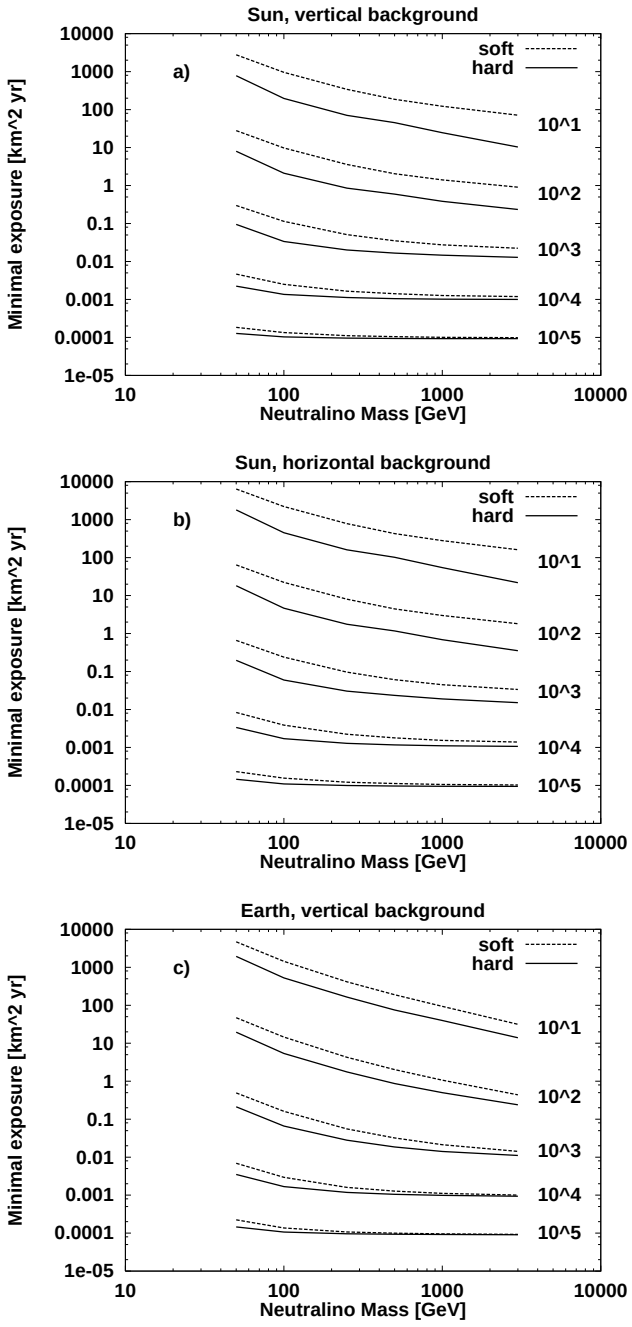

FIG. 1. The exposures needed for a 3σ discovery for different signal fluxes (indicated to the right in the figure in units of km^{-2} yr^{-1}) as a function of WIMP mass assuming perfect angular resolution but no energy resolution (and with a muon energy threshold of 1 GeV). The three figures correspond to annihilation in a) the Sun with vertical background, b) the Sun with horizontal background and c) the Earth with vertical background. The solid(dashed) lines correspond to soft(hard) muon spectra. The three signal parameters $\{\phi_s^0, m_\chi, a\}$ in Eq. (3) are assumed to be unknown while the background flux is assumed to be known. Note that only exposures less than, say, 25 km^{-2} yr^{-1} are realistic in the near future.

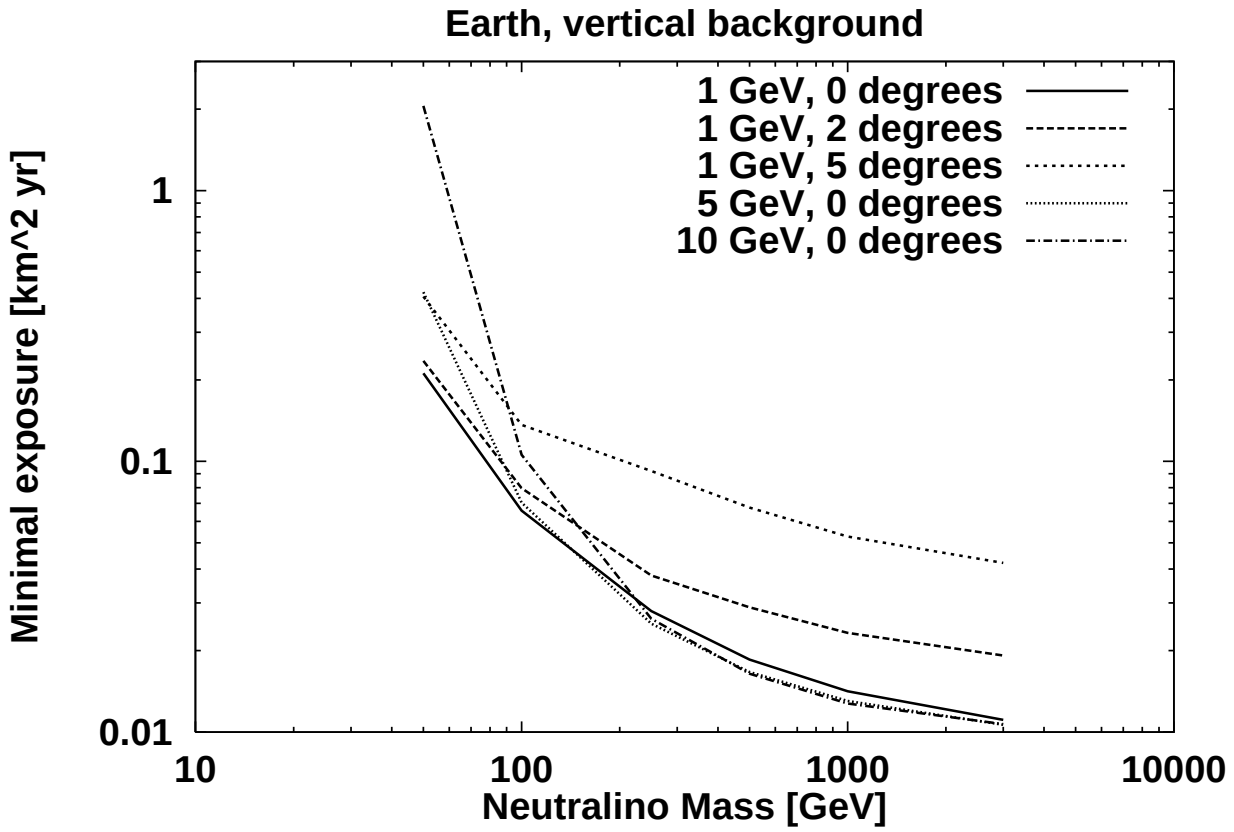

FIG. 2. The exposures needed for a 3σ discovery for the signal flux $\phi_s^0 = 10^3$ km^{-2} yr^{-1} coming from WIMP annihilation in the Earth. The three signal parameters $\{\phi_s^0, m_\chi, a\}$ in Eq. (3) are assumed to be unknown while the background flux is assumed to be known. The change of the minimal exposures needed when changing the experimental angular resolution or increasing the energy threshold is indicated. All curves are for hard annihilation spectra.

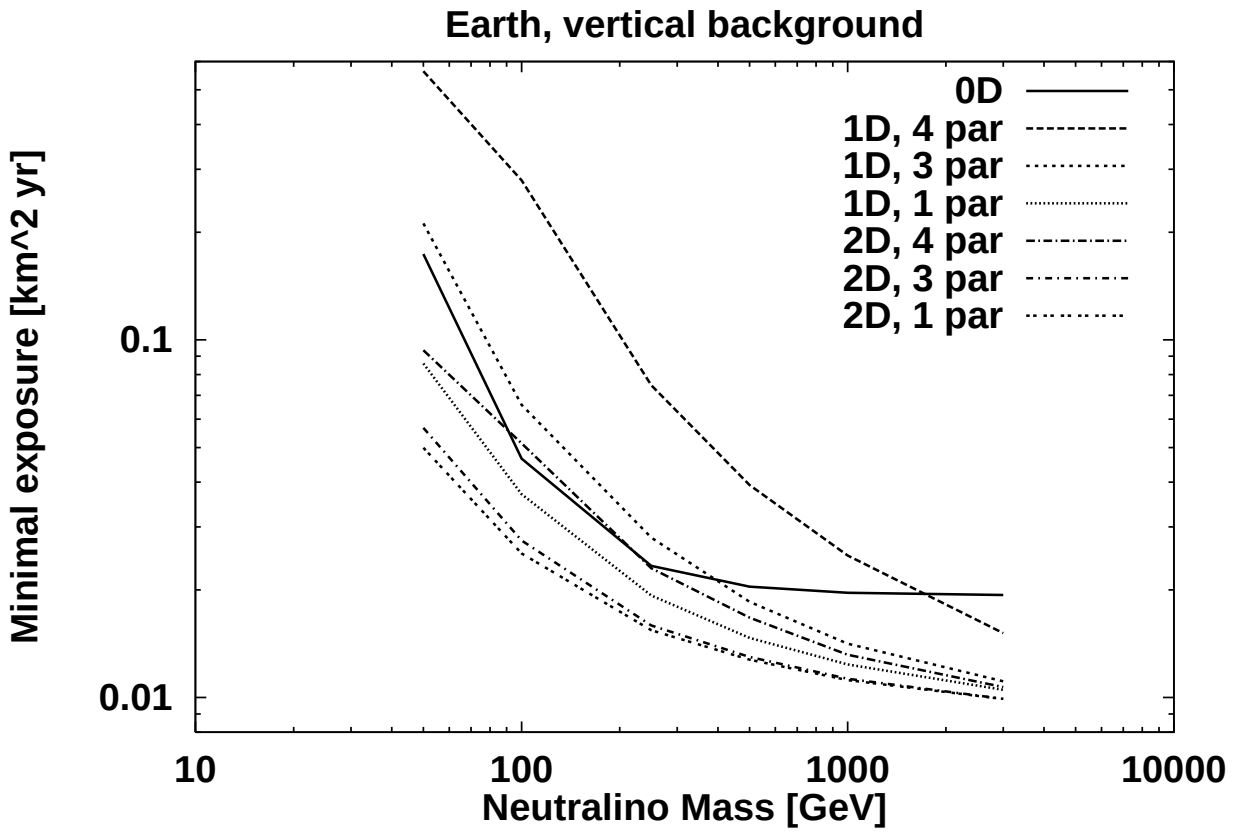

FIG. 3. The exposures needed for a 3σ discovery for the signal flux $\phi_s^0 = 10^3$ km^{-2} yr^{-1} coming from WIMP annihilation in the Earth. The minimal exposures needed for a detector with neither angular nor energy resolution (0D), only angular but no energy resolution (1D) and both angular and energy resolution (2D) is shown. For the 1D and 2D cases, results are given for all four parameters in Eqs. (2) and (3) being free (4 par), only the three signal flux parameters being free (3 par) and only the normalization of the signal flux, ϕ_s^0 being free (1 par). An energy threshold of 1 GeV is used in all cases and for the 0D case an integration of the fluxes up to $\theta_{\rm max} = 5^\circ$ is performed. All curves are for hard annihilation spectra.

of the 4-parameter curves all depend on the upper limit of the θ-integration since the higher it is, the more background is included in the fit and the lower the curves get. If we compare the improvement by using the 3-parameter fit for the signal to the simple case of using just one bin up to a certain angle $\theta_{\rm max}$ we see that the minimal exposures needed are of the same order for small masses while there is an improvement of up to a factor of 2 at higher masses. Note however that with the 3-parameter approach we will also gain some information on the mass and hardness of the spectrum. Also, a problem with the single bin approach is the choice of $\theta_{\rm max}$. If we choose $\theta_{\rm max} < 5^\circ$ we could get the single bin curve and the 3-parameter angular resolution curve to match at high masses but then the single bin curve would do much worse at low masses. At low masses ($\lesssim 100$ GeV) the optimum choice would be more than 5° and at high masses less. We cannot however know in beforehand what the optimum choice is. This problem we avoid by using the signal flux parameterization, Eq (3), proposed here and get about the same sensitivity as with the single bin approach with optimal $\theta_{\rm max}$.

If we are interested only in looking for a nonzero signal flux ϕ_s^0 for some specific hypothesized WIMP mass and neutrino spectrum, we gain about a factor of 1–1.5 more and will always do better than the one-bin approach. This might be the case if the WIMP is found at accelerators and we know its properties but want to know if it constitutes the dark matter in the Universe.

We can conclude from Fig. 1 and Tables I–III that a reasonable detector with perfect angular resolution and exposures in the order of 1–25 km^2 yr would be able to detect signal fluxes down to about 100 km^{-2} yr^{-1} (slightly more at low masses and slightly less at high masses).

B. Detector with angular resolution and variable energy threshold

Our next case to consider is a neutrino telescope with perfect angular resolution and variable muon energy thresholds. This may be achieved by, e.g., using different triggering conditions. By increasing the energy threshold we expect to increase the signal-to-noise ratio (at least if the threshold is well below the WIMP mass) and hence get better signal detection possibilities. Of course, it would be even better to have full energy resolution (as described in the next subsection). However, the energy resolution of current neutrino detectors is not great, but changing the threshold might be a good option.

We have chosen to evaluate the needed minimal exposures for the muon energy thresholds $E_\mu^{th} = 1$, 5, 10, 25, 50, and 100 GeV and in Fig. 2 we show the minimal exposures needed for detection for muon energy thresholds of 5 and 10 GeV compared to the threshold of 1 GeV for WIMP annihilation in the Earth. The general trend for annihilation in the Sun and for other signal fluxes are the same as those shown in the figure, namely that there is a small gain by increasing the threshold when the WIMP mass is above 100 GeV but below too much signal is also lost and the needed minimal exposures are higher. At thresholds of 25, 50, and 100 GeV, the needed minimal exposures are higher than or about the same as with a threshold of 10 GeV. Hence there is no gain with increasing the threshold higher than to about 10 GeV.

To conclude on varying the threshold, the gain is very small and only for WIMP masses above 100 GeV. Increasing the threshold above 10 GeV gives no further improvements. On

the other hand, large detectors (like AMANDA) which have a threshold of tens of GeV will not lose much sensitivity either, for WIMP masses above 100 GeV.

C. Detector with angular and energy resolution

If we imagine a detector where we have both perfect angular and energy resolution, what improvement in minimal exposures do we get? In Fig. 3 we compare the minimal exposures needed for such a detector and a detector with only angular resolution. We also compare with the simple case of just having one bin in angle. The improvement by having both energy and angular resolution compared to just having angular resolution can be as high as a factor of 2 at low WIMP masses, but at higher masses the improvement is less. However, if the signal flux is small the improvement is of about a factor of 2 at all masses and if the signal flux is high, the improvement is small for all masses.

Since supersymmetric models generally predict relatively low fluxes [1,2], this improvement could be significant.

D. Example of a neutrino detector

Let us consider a detector with a size of MACRO (effective area about 650 m^2 towards the Sun). What improvements can be done with such a detector by using only angular or both the angular and energy resolution. Assume that the exposure towards the Sun is $\mathcal{E} = 5000$ km^2 yr (about 15 years of data taking and the Sun being below the horizon for 50% of the time) and that the atmospheric background is vertical. In Fig. 4 we show a comparison between having only one bin, having perfect angular resolution and having both perfect angular and energy resolution. The signal fluxes that are given here are for hard muon fluxes. When the fluxes are soft, the curves are higher. In (a), we show results for the case when we have a given hypothesis, i.e. a WIMP of a given mass and a given composition. Hence we compare the one-bin approach with optimal $\theta_{\max}$ (for the given hypothesis) with the case of angular and/or energy resolution where only ϕ_s^0 is kept free. In (b), we show results when our hypothesis is that we look for WIMPs with masses up to 3000 GeV and with different composition. Hence we compare results for $\theta_{\max} = 5^\circ$ and all three signal parameters $\{\phi_s^0, m_\chi, a\}$ in Eq. (3) being unknown. We see clearly that at high masses, there is a substantial gain by having perfect angular resolution (at what masses the gain is highest depends on $\theta_{\max}$) and especially at low masses there is a substantial gain by having perfect energy resolution as well.

Note that in this example we are almost in the signal dominated regime so that by increasing the exposure, $\mathcal{E}$, by a small factor, we decrease the limit on ϕ_s^0 by almost the same amount, especially at high masses.

E. Discussion

From our results earlier in this Section we see that for the neutrino signal coming from WIMP annihilations in the Sun and in the Earth we gain about a factor of 2 at high masses

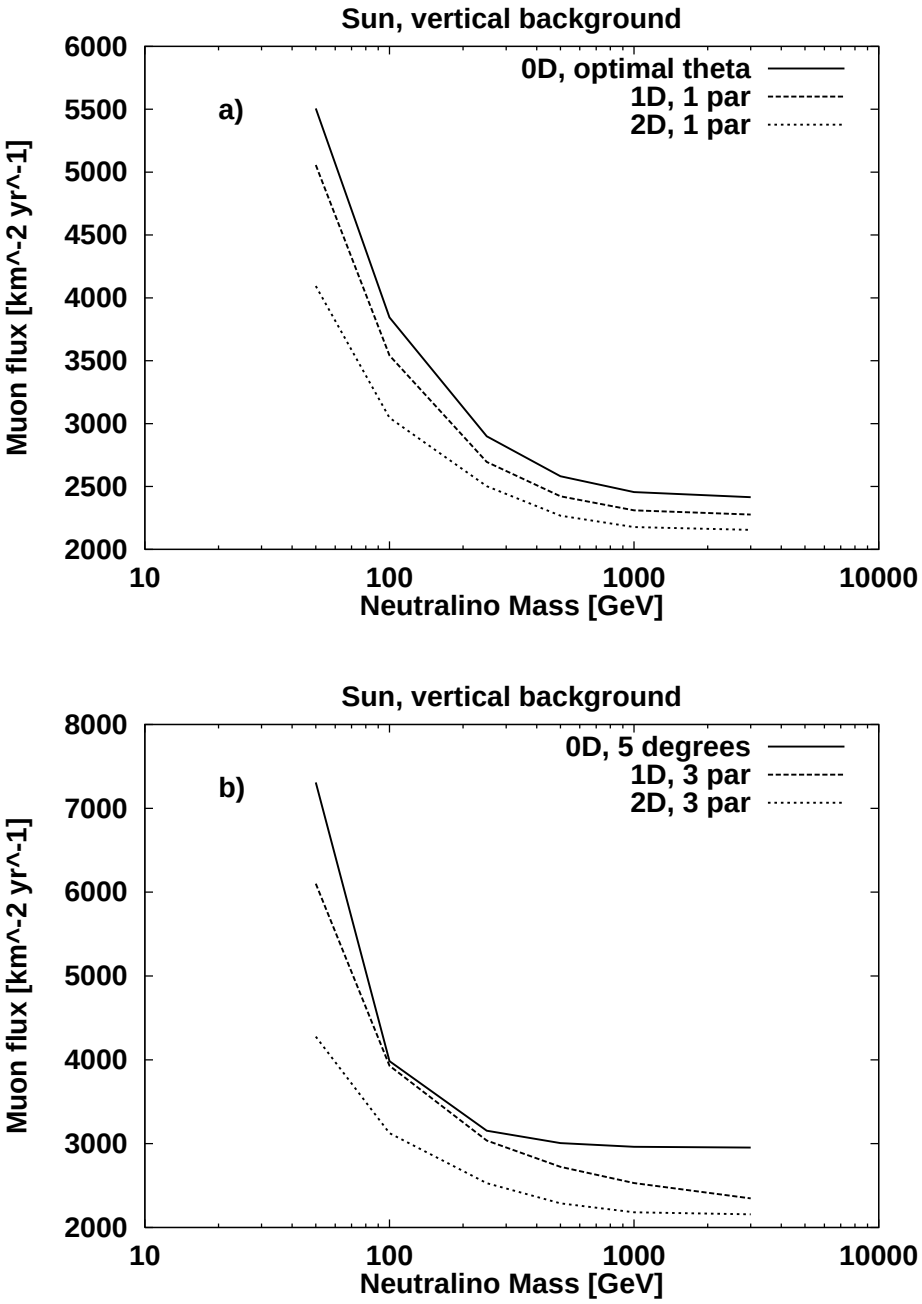

FIG. 4. The muon fluxes (coming from WIMP annihilations in the Sun) that can be discovered (at the 3σ level) when the WIMP spectrum is hard with the exposure $\mathcal{E} = 0.005$ km^2 yr. The different cases of only having one angular bin (0D), having perfect angular resolution (1D) and having perfect angular and energy resolution (2D) are compared. In a) the optimal $\theta_{\rm max}$ for each mass is used in the 0D case and only ϕ_s^0 is assumed to be unknown for the 1D and 2D cases and in b) $\theta_{\rm max} = 5^\circ$ is used in the 0D case and all three signal parameters $\{\phi_s^0, m_\chi, a\}$ in Eq. (3) are assumed to be unknown in the 1D and 2D cases. In both a) and b) the background flux is assumed to be known and the atmospheric background is assumed to be vertical.

by using the angular resolution of a neutrino telescope. At lower masses there is hardly any difference to the simple approach of just having one bin up to a certain maximum angle $\theta_{\max}$, but at higher masses there is a significant difference. Note however that how well the single-bin approach does at different masses depends on $\theta_{\max}$ as described in Section III A. Note also that by using the parameterization of the signal flux proposed here we can also gain some information on the WIMP mass and the hardness of the spectrum.

By varying the energy threshold not much more is gained, but by having energy resolution about a factor of 1.5–2 can be gained, slightly more at low signal fluxes and slightly less at high signal fluxes.

We can also note that for neutrino telescopes in the size of about 1 km^2 the signal fluxes we can expect to probe is in the region of 50–100 km^{-2} yr^{-1} with a neutrino telescope with angular resolution and slightly less for a telescope with also energy resolution. Hence the signal fluxes within reach are almost an order of magnitude larger than the expected background coming from cosmic ray interactions in the Sun (about 15 events km^{-2} yr^{-1} [17]). Therefore it is quite safe to neglect this background at the present stage. When detectors are getting even bigger it will however be a severe limitation when looking for the neutrino flux from the Sun since this background is also highly directional as the signal. Note, though, that the energy dependence is expected to be quite different, so having energy resolution may be quite beneficial in this case.

IV. CONCLUSIONS

We have evaluated the improvement in sensitivity to astrophysical neutrino point sources that can be achieved with muon resolution and with muon energy resolution. We have focused on neutrinos from WIMP annihilation in the Sun and Earth and considered WIMP candidates with a variety of masses and neutrino spectra. For example, for detectors with exposures comparable to Baksan, Kamiokande II, and/or MACRO, an analysis which uses angular information can improve the sensitivity to neutrinos from annihilation of WIMPs in the Sun and Earth by 10–40%, depending on whether the backgrounds are vertical or horizontal. Energy resolution could improve the sensitivity by roughly another 10–65%. Angular and energy resolution generally provides an improvement in sensitivity to signals which are small (approaching the inverse exposure of the detector). We have shown that with a 1 km^2 neutrino telescope it is possible to probe muon fluxes coming from WIMP annihilation in the Sun and Earth down to about 50–100 km^{-2} yr^{-1}. For detector with an exposure comparable to that of MACRO after 15 years, energy resolution could in some cases reduce the atmospheric-neutrino background to insignificant levels.

Currently, the primary issue in dark-matter detection is discovery, so we have focused here on how the sensitivity to neutrinos from WIMP annihilation can be improved from energy and angular resolution. However, directional and energy information will also be useful for other reasons as well. For example, in case of a positive detection, the angular distribution of the muons from the Sun/Earth can be used to infer the mass of the WIMP [18]. If there is also energy resolution, this mass determination can be made increasingly precise, and one might also be able to infer something about the neutrino energy distribution. Although we have not carried out the calculation, the covariance-matrix formalism described in Section

II can be used to evaluate the accuracies with which the WIMP mass can be measured for various WIMP candidates and with various experimental configurations. Of course, the method developed here can be used the determine the sensitivity to other point sources of neutrinos as well. Energy resolution will also be essential for studying, for example, more conventional astrophysical point sources of neutrinos and atmospheric neutrinos.

The angular resolution of current experiments is already quite good, and this information should be used to improve the sensitivity to neutrinos from dark-matter annihilation. Although current experiments do not have good energy resolution (or any energy resolution at all), there are indeed ideas for obtaining some estimates of the energy, and ideas for future experiments with fairly precise energy resolution are currently being explored. We hope that the work presented here will help spur new ideas for experimental determination of the muon energy in neutrino telescopes.

ACKNOWLEDGMENTS

LB was supported by the Swedish Natural Science Research Council (NFR). MK was supported in part by the D.O.E. under contract DEFG02-92-ER 40699, NASA under contract NAG5-3091, and by the Alfred P. Sloan Foundation. MK acknowledges the hospitality of the Theory Division at CERN, where part of this work was completed. MK also acknowledges the hospitality of the Uppsala/NORDITA Astroparticle Workshop where this work was initiated. MK thanks Wonyong Lee for useful discussions.

REFERENCES

[1] J. Silk, K. Olive, and M. Srednicki, Phys. Rev. Lett. **55** (1985) 257; K. Freese, Phys. Lett. **B167** (1986) 295; L. M. Krauss, K. Freese, D. N. Spergel, and W. H. Press, Astrophys. J. **299** (1985) 1001; L. M. Krauss, M. Srednicki, and F. Wilczek, Phys. Rev. **D33** (1986) 2079; T. Gaisser, G. Steigman, and S. Tilav, Phys. Rev. **D34** (1986) 2206; M. Kamionkowski, Phys. Rev. **D44** (1991) 3021; V. Berezinskii, A. Bottino, J. Ellis, N. Fornengo, G. Mignola and S. Scopel, Astropart. Phys. **5** (1996) 333; L. Bergström, J. Edsjö, and P. Gondolo, hep-ph/9607237, Phys. Rev. **D**, in press.

[2] G. Jungman, M. Kamionkowski and K. Griest, Phys. Rep. **267** (1996) 195.

[3] M.M. Boliev et al., Bull. Acad. Sci. USSR, Phys. Ser. **55** (1991) 126 [Izv. Akad. Nauk. SSSR, Fiz. **55** (1991) 748]; M.M. Boliev et al., in *TAUP 95*, proceedings of the Workshop, Toledo, Spain, September 17–21, 1995, edited by A. Morales, J. Morales and J.A. Villar, [Nucl. Phys. (Proc. Suppl.) **B48** (1996) 83] (North-Holland, Amsterdam, 1996).

[4] J. M. LoSecco et al. (IMB Collaboration), Phys. Lett. **B188** (1987) 388.

[5] M. Mori et al. (Kamiokande Collaboration), Phys. Lett. **B289** (1992) 463; M. Mori et al. (Kamiokande Collaboration), Phys. Rev. **D48** (1993) 5505.

[6] E. Diehl, Ph.D. Thesis, U. of Michigan (1994).

[7] Frejus Collaboration, presented by H. J. Daum, Topical Seminar on Astrophysics and Particle Physics, San Miniato, Italy, 1989.

[8] Y. Totsuka, in *TAUP 95*, proceedings of the Workshop, Toledo, Spain, September 17–21, 1995, edited by A. Morales, J. Morales and J.A. Villar, [Nucl. Phys. (Proc. Suppl.) **B48** (1996) 547].

[9] P.O. Hulth et al (AMANDA Collaboration), to be published in Proceedings of the XVII International Conference in Neutrino Physics and Astrophysics, Neutrino 96, Helsinki, Finland 13-19 June 1996, eds. K. Enqvist, K. Huitu and J. Maalampi (World Scientific, Singapore, 1997).

[10] L. Resvanis, Europhys. News **23** (1992) 172.

[11] W. Lee, private communication.

[12] S. Ritz and D. Seckel, Nucl. Phys. **B304** (1988) 877; G. Jungman and M. Kamionkowski, Phys. Rev. **D51** (1995) 328.

[13] J. Edsjö, in *Trends in Astroparticle Physics*, proceedings of the Workshop, Stockholm, Sweden, September 22–25, 1994, edited by L. Bergström, P. Carlson, P.O. Hulth, and H. Snellman, [Nucl. Phys. (Proc. Suppl.) **B43** (1995) 265] (North-Holland, Amsterdam, 1995).

[14] A. Bottino, N. Fornengo, G. Mignola and L. Moscoso, Astropart. Phys. **3** (1995) 65.

[15] A. Bottino et al., Astropart. Phys. **2** (1994) 77.

[16] M. Honda et al., Phys. Rev. **D52** (1995) 4985.

[17] D. Seckel, T. Stanev and T.K. Gaisser, Astrophys. J. **382** (1991) 651; G. Ingelman and M. Thunman, Phys. Rev. **D54** (1996) 4385.

[18] J. Edsjö and P. Gondolo, Phys. Lett. **B357** (1995) 595.

APPENDIX A: TABLES OF MINIMAL EXPOSURES

Below are tables giving minimal exposures needed for a 3σ discovery of the neutrino signal coming from WIMP annihilation in the Sun and Earth. The column labeled "OD" refers to an experiment with a 1-GeV muon threshold but with no further energy or angular resolution. The columns labeled "1D" refer to experiments with angular but no energy resolution, and those labeled "2D" refer to experiments with both energy and angular resolution. The column labeled "4par" gives the minimum exposure needed for a 3σ detection of the source flux after marginalizing over the unknown WIMP mass (m_χ), background flux (ϕ_s^0), and "hardness" (a) of the source spectrum. The column labeled "3par" gives the minimum exposure needed for a 3σ detection of the source flux assuming the background flux is known from, e.g., off-source measurements, but after marginalizing over the unknown WIMP mass and "hardness" of the source spectrum. The column labeled "1par" gives the minimum exposure needed for a 3σ detection of the source flux for a fixed WIMP mass, source-spectrum hardness, and background flux.

Note that if interpolations in the tables are needed, they should be done on the logarithms of ϕ_s^0 and $\mathcal{E}_{\rm min}$. For smaller signal fluxes than those given here, $\mathcal{E}_{\rm min}$ scale such that lowering the signal flux a factor of 10 increases $\mathcal{E}_{\rm min}$ by a factor of 100.

ϕ_s^0 [km^{-2} yr^{-1}]	m_χ [GeV]	$\mathcal{E}_{\rm min}^{\rm 0D}$ [km^2 yr]	$\mathcal{E}_{\rm min}^{\rm 1D,4par}$ [km^2 yr]	$\mathcal{E}_{\rm min}^{\rm 1D,3par}$ [km^2 yr]	$\mathcal{E}_{\rm min}^{\rm 1D,1par}$ [km^2 yr]	$\mathcal{E}_{\rm min}^{\rm 2D,3par}$ [km^2 yr]	$\mathcal{E}_{\rm min}^{\rm 2D,1par}$ [km^2 yr]
1.0×10^{0}	50	7.3×10^{4}	3.1×10^{5}	7.8×10^{4}	4.8×10^{4}	2.1×10^{4}	1.9×10^{4}
1.0×10^{0}	100	2.0×10^{4}	1.0×10^{5}	2.0×10^{4}	1.4×10^{4}	6.1×10^{3}	5.4×10^{3}
1.0×10^{0}	250	1.2×10^{4}	3.5×10^{4}	6.9×10^{3}	3.7×10^{3}	1.4×10^{3}	1.3×10^{3}
1.0×10^{0}	500	1.1×10^{4}	1.9×10^{4}	4.4×10^{3}	1.7×10^{3}	5.4×10^{2}	5.1×10^{2}
1.0×10^{0}	1000	1.1×10^{4}	9.8×10^{3}	2.3×10^{3}	1.1×10^{3}	2.8×10^{2}	2.8×10^{2}
1.0×10^{0}	3000	1.1×10^{4}	8.8×10^{3}	8.9×10^{2}	8.1×10^{2}	1.9×10^{2}	1.9×10^{2}
1.0×10^{1}	50	7.3×10^{2}	3.1×10^{3}	7.8×10^{2}	4.8×10^{2}	2.1×10^{2}	1.9×10^{2}
1.0×10^{1}	100	2.0×10^{2}	1.0×10^{3}	2.0×10^{2}	1.4×10^{2}	6.3×10^{1}	5.6×10^{1}
1.0×10^{1}	250	1.3×10^{2}	3.5×10^{2}	7.1×10^{1}	3.8×10^{1}	1.6×10^{1}	1.5×10^{1}
1.0×10^{1}	500	1.1×10^{2}	1.8×10^{2}	4.5×10^{1}	1.8×10^{1}	7.4×10^{0}	7.2×10^{0}
1.0×10^{1}	1000	1.1×10^{2}	1.0×10^{2}	2.5×10^{1}	1.2×10^{1}	4.9×10^{0}	4.9×10^{0}
1.0×10^{1}	3000	1.1×10^{2}	8.9×10^{1}	1.0×10^{1}	9.8×10^{0}	4.1×10^{0}	4.1×10^{0}
1.0×10^{2}	50	7.5×10^{0}	3.1×10^{1}	8.0×10^{0}	4.9×10^{0}	2.3×10^{0}	2.1×10^{0}
1.0×10^{2}	100	2.1×10^{0}	1.0×10^{1}	2.1×10^{0}	1.5×10^{0}	8.0×10^{-1}	7.3×10^{-1}
1.0×10^{2}	250	1.3×10^{0}	3.8×10^{0}	8.6×10^{-1}	5.1×10^{-1}	3.1×10^{-1}	3.0×10^{-1}
1.0×10^{2}	500	1.2×10^{0}	2.1×10^{0}	6.0×10^{-1}	3.2×10^{-1}	2.2×10^{-1}	2.1×10^{-1}
1.0×10^{2}	1000	1.2×10^{0}	1.1×10^{0}	3.8×10^{-1}	2.6×10^{-1}	1.8×10^{-1}	1.8×10^{-1}
1.0×10^{2}	3000	1.2×10^{0}	1.0×10^{0}	2.3×10^{-1}	2.3×10^{-1}	1.7×10^{-1}	1.7×10^{-1}
1.0×10^{3}	50	9.7×10^{-2}	3.3×10^{-1}	9.5×10^{-2}	6.2×10^{-2}	3.8×10^{-2}	3.6×10^{-2}
1.0×10^{3}	100	3.2×10^{-2}	1.3×10^{-1}	3.4×10^{-2}	2.7×10^{-2}	2.1×10^{-2}	2.0×10^{-2}
1.0×10^{3}	250	2.2×10^{-2}	5.4×10^{-2}	2.0×10^{-2}	1.6×10^{-2}	1.4×10^{-2}	1.4×10^{-2}
1.0×10^{3}	500	2.1×10^{-2}	3.6×10^{-2}	1.7×10^{-2}	1.4×10^{-2}	1.2×10^{-2}	1.2×10^{-2}
1.0×10^{3}	1000	2.0×10^{-2}	2.3×10^{-2}	1.5×10^{-2}	1.3×10^{-2}	1.2×10^{-2}	1.2×10^{-2}
1.0×10^{3}	3000	2.0×10^{-2}	2.0×10^{-2}	1.3×10^{-2}	1.2×10^{-2}	1.1×10^{-2}	1.1×10^{-2}
1.0×10^{4}	50	3.1×10^{-3}	5.0×10^{-3}	2.2×10^{-3}	1.7×10^{-3}	1.5×10^{-3}	1.4×10^{-3}
1.0×10^{4}	100	1.5×10^{-3}	2.6×10^{-3}	1.4×10^{-3}	1.3×10^{-3}	1.2×10^{-3}	1.1×10^{-3}
1.0×10^{4}	250	1.1×10^{-3}	1.6×10^{-3}	1.1×10^{-3}	1.1×10^{-3}	1.1×10^{-3}	1.0×10^{-3}
1.0×10^{4}	500	1.1×10^{-3}	1.3×10^{-3}	1.1×10^{-3}	1.0×10^{-3}	9.9×10^{-4}	9.9×10^{-4}
1.0×10^{4}	1000	1.0×10^{-3}	1.1×10^{-3}	1.0×10^{-3}	9.9×10^{-4}	9.8×10^{-4}	9.8×10^{-4}
1.0×10^{4}	3000	1.0×10^{-3}	1.1×10^{-3}	1.0×10^{-3}	9.9×10^{-4}	9.7×10^{-4}	9.7×10^{-4}
1.0×10^{5}	50	2.5×10^{-4}	1.7×10^{-4}	1.3×10^{-4}	1.1×10^{-4}	1.1×10^{-4}	1.1×10^{-4}
1.0×10^{5}	100	1.3×10^{-4}	1.2×10^{-4}	1.0×10^{-4}	1.0×10^{-4}	9.9×10^{-5}	9.9×10^{-5}
1.0×10^{5}	250	1.0×10^{-4}	1.0×10^{-4}	9.6×10^{-5}	9.5×10^{-5}	9.6×10^{-5}	9.6×10^{-5}
1.0×10^{5}	500	9.6×10^{-5}	9.8×10^{-5}	9.4×10^{-5}	9.3×10^{-5}	9.3×10^{-5}	9.3×10^{-5}
1.0×10^{5}	1000	9.4×10^{-5}	9.5×10^{-5}	9.3×10^{-5}	9.3×10^{-5}	9.2×10^{-5}	9.2×10^{-5}
1.0×10^{5}	3000	9.4×10^{-5}	9.4×10^{-5}	9.3×10^{-5}	9.2×10^{-5}	9.2×10^{-5}	9.2×10^{-5}

TABLE I. The minimal exposures needed to make a 3σ discovery of WIMP annihilation in the Sun when the atmospheric background is vertical. The values given are for hard muon spectra and a muon energy threshold of 1 GeV.

ϕ_s^0 [km^{-2} yr^{-1}]	m_χ [GeV]	$\mathcal{E}_{\rm min}^{\rm 0D}$ [km^2 yr]	$\mathcal{E}_{\rm min}^{\rm 1D,4par}$ [km^2 yr]	$\mathcal{E}_{\rm min}^{\rm 1D,3par}$ [km^2 yr]	$\mathcal{E}_{\rm min}^{\rm 1D,1par}$ [km^2 yr]	$\mathcal{E}_{\rm min}^{\rm 2D,3par}$ [km^2 yr]	$\mathcal{E}_{\rm min}^{\rm 2D,1par}$ [km^2 yr]
1.0×10^{0}	50	1.7×10^{5}	7.2×10^{5}	1.8×10^{5}	1.1×10^{5}	4.7×10^{4}	4.3×10^{4}
1.0×10^{0}	100	4.6×10^{4}	2.3×10^{5}	4.5×10^{4}	3.2×10^{4}	1.5×10^{4}	1.3×10^{4}
1.0×10^{0}	250	2.9×10^{4}	8.0×10^{4}	1.6×10^{4}	8.4×10^{3}	3.8×10^{3}	3.4×10^{3}
1.0×10^{0}	500	2.6×10^{4}	4.2×10^{4}	1.0×10^{4}	3.8×10^{3}	1.4×10^{3}	1.4×10^{3}
1.0×10^{0}	1000	2.5×10^{4}	2.3×10^{4}	5.3×10^{3}	2.5×10^{3}	7.7×10^{2}	7.7×10^{2}
1.0×10^{0}	3000	2.5×10^{4}	2.0×10^{4}	2.0×10^{3}	1.8×10^{3}	5.3×10^{2}	5.2×10^{2}
1.0×10^{1}	50	1.7×10^{3}	7.2×10^{3}	1.8×10^{3}	1.1×10^{3}	4.7×10^{2}	4.3×10^{2}
1.0×10^{1}	100	4.6×10^{2}	2.4×10^{3}	4.5×10^{2}	3.2×10^{2}	1.5×10^{2}	1.3×10^{2}
1.0×10^{1}	250	2.9×10^{2}	8.0×10^{2}	1.6×10^{2}	8.6×10^{1}	4.0×10^{1}	3.6×10^{1}
1.0×10^{1}	500	2.6×10^{2}	4.2×10^{2}	1.0×10^{2}	4.0×10^{1}	1.7×10^{1}	1.6×10^{1}
1.0×10^{1}	1000	2.5×10^{2}	2.2×10^{2}	5.5×10^{1}	2.7×10^{1}	1.0×10^{1}	1.0×10^{1}
1.0×10^{1}	3000	2.5×10^{2}	2.0×10^{2}	2.2×10^{1}	2.0×10^{1}	7.7×10^{0}	7.7×10^{0}
1.0×10^{2}	50	1.7×10^{1}	7.2×10^{1}	1.8×10^{1}	1.1×10^{1}	4.9×10^{0}	4.5×10^{0}
1.0×10^{2}	100	4.7×10^{0}	2.4×10^{1}	4.7×10^{0}	3.3×10^{0}	1.6×10^{0}	1.5×10^{0}
1.0×10^{2}	250	3.0×10^{0}	8.3×10^{0}	1.8×10^{0}	1.0×10^{0}	5.6×10^{-1}	5.2×10^{-1}
1.0×10^{2}	500	2.7×10^{0}	4.5×10^{0}	1.2×10^{0}	5.4×10^{-1}	3.3×10^{-1}	3.2×10^{-1}
1.0×10^{2}	1000	2.6×10^{0}	2.4×10^{0}	6.9×10^{-1}	4.1×10^{-1}	2.6×10^{-1}	2.6×10^{-1}
1.0×10^{2}	3000	2.6×10^{0}	2.1×10^{0}	3.5×10^{-1}	3.5×10^{-1}	2.4×10^{-1}	2.4×10^{-1}
1.0×10^{3}	50	1.9×10^{-1}	7.4×10^{-1}	2.0×10^{-1}	1.2×10^{-1}	6.5×10^{-2}	6.0×10^{-2}
1.0×10^{3}	100	5.8×10^{-2}	2.6×10^{-1}	6.0×10^{-2}	4.5×10^{-2}	3.1×10^{-2}	2.9×10^{-2}
1.0×10^{3}	250	3.8×10^{-2}	1.0×10^{-1}	3.0×10^{-2}	2.2×10^{-2}	1.8×10^{-2}	1.7×10^{-2}
1.0×10^{3}	500	3.5×10^{-2}	6.4×10^{-2}	2.4×10^{-2}	1.7×10^{-2}	1.5×10^{-2}	1.4×10^{-2}
1.0×10^{3}	1000	3.5×10^{-2}	3.8×10^{-2}	1.9×10^{-2}	1.5×10^{-2}	1.3×10^{-2}	1.3×10^{-2}
1.0×10^{3}	3000	3.4×10^{-2}	3.2×10^{-2}	1.5×10^{-2}	1.5×10^{-2}	1.3×10^{-2}	1.3×10^{-2}
1.0×10^{4}	50	4.1×10^{-3}	9.3×10^{-3}	3.4×10^{-3}	2.4×10^{-3}	1.9×10^{-3}	1.8×10^{-3}
1.0×10^{4}	100	1.7×10^{-3}	4.2×10^{-3}	1.7×10^{-3}	1.5×10^{-3}	1.3×10^{-3}	1.3×10^{-3}
1.0×10^{4}	250	1.3×10^{-3}	2.2×10^{-3}	1.3×10^{-3}	1.2×10^{-3}	1.1×10^{-3}	1.1×10^{-3}
1.0×10^{4}	500	1.2×10^{-3}	1.7×10^{-3}	1.2×10^{-3}	1.1×10^{-3}	1.1×10^{-3}	1.0×10^{-3}
1.0×10^{4}	1000	1.2×10^{-3}	1.4×10^{-3}	1.1×10^{-3}	1.0×10^{-3}	1.0×10^{-3}	1.0×10^{-3}
1.0×10^{4}	3000	1.2×10^{-3}	1.2×10^{-3}	1.1×10^{-3}	1.0×10^{-3}	1.0×10^{-3}	1.0×10^{-3}
1.0×10^{5}	50	2.6×10^{-4}	2.3×10^{-4}	1.5×10^{-4}	1.2×10^{-4}	1.2×10^{-4}	1.1×10^{-4}
1.0×10^{5}	100	1.3×10^{-4}	1.5×10^{-4}	1.1×10^{-4}	1.1×10^{-4}	1.0×10^{-4}	1.0×10^{-4}
1.0×10^{5}	250	1.0×10^{-4}	1.1×10^{-4}	9.9×10^{-5}	9.8×10^{-5}	9.8×10^{-5}	9.8×10^{-5}
1.0×10^{5}	500	9.7×10^{-5}	1.0×10^{-4}	9.6×10^{-5}	9.5×10^{-5}	9.5×10^{-5}	9.4×10^{-5}
1.0×10^{5}	1000	9.6×10^{-5}	9.9×10^{-5}	9.5×10^{-5}	9.4×10^{-5}	9.4×10^{-5}	9.4×10^{-5}
1.0×10^{5}	3000	9.5×10^{-5}	9.7×10^{-5}	9.4×10^{-5}	9.4×10^{-5}	9.3×10^{-5}	9.3×10^{-5}

TABLE II. The minimal exposures needed to make a 3σ discovery of WIMP annihilation in the Sun when the atmospheric background is horizontal. The values given are for hard muon spectra and a muon energy threshold of 1 GeV.

ϕ_s^0 [km^{-2} yr^{-1}]	m_χ [GeV]	$\mathcal{E}_{\rm min}^{\rm 0D}$ [km^2 yr]	$\mathcal{E}_{\rm min}^{\rm 1D,4par}$ [km^2 yr]	$\mathcal{E}_{\rm min}^{\rm 1D,3par}$ [km^2 yr]	$\mathcal{E}_{\rm min}^{\rm 1D,1par}$ [km^2 yr]	$\mathcal{E}_{\rm min}^{\rm 2D,3par}$ [km^2 yr]	$\mathcal{E}_{\rm min}^{\rm 2D,1par}$ [km^2 yr]
1.0×10^{0}	50	1.4×10^{5}	5.2×10^{5}	1.9×10^{5}	7.2×10^{4}	3.9×10^{4}	3.4×10^{4}
1.0×10^{0}	100	3.1×10^{4}	2.5×10^{5}	5.2×10^{4}	2.4×10^{4}	1.3×10^{4}	1.1×10^{4}
1.0×10^{0}	250	1.3×10^{4}	5.7×10^{4}	1.6×10^{4}	7.6×10^{3}	3.3×10^{3}	3.0×10^{3}
1.0×10^{0}	500	1.1×10^{4}	2.5×10^{4}	7.4×10^{3}	3.5×10^{3}	1.4×10^{3}	1.2×10^{3}
1.0×10^{0}	1000	1.1×10^{4}	1.4×10^{4}	3.9×10^{3}	1.7×10^{3}	4.7×10^{2}	3.9×10^{2}
1.0×10^{0}	3000	1.0×10^{4}	4.8×10^{3}	1.3×10^{3}	5.2×10^{2}	6.8×10^{2}	6.2×10^{1}
1.0×10^{1}	50	1.4×10^{3}	5.2×10^{3}	1.9×10^{3}	7.3×10^{2}	3.9×10^{2}	3.4×10^{2}
1.0×10^{1}	100	3.1×10^{2}	2.5×10^{3}	5.3×10^{2}	2.4×10^{2}	1.3×10^{2}	1.1×10^{2}
1.0×10^{1}	250	1.3×10^{2}	5.8×10^{2}	1.6×10^{2}	7.7×10^{1}	3.5×10^{1}	3.1×10^{1}
1.0×10^{1}	500	1.1×10^{2}	2.5×10^{2}	7.5×10^{1}	3.7×10^{1}	1.5×10^{1}	1.3×10^{1}
1.0×10^{1}	1000	1.1×10^{2}	1.4×10^{2}	4.0×10^{1}	1.8×10^{1}	6.5×10^{0}	5.6×10^{0}
1.0×10^{1}	3000	1.0×10^{2}	4.9×10^{1}	1.4×10^{1}	6.5×10^{0}	2.3×10^{0}	2.1×10^{0}
1.0×10^{2}	50	1.4×10^{1}	5.3×10^{1}	2.0×10^{1}	7.4×10^{0}	4.1×10^{0}	3.5×10^{0}
1.0×10^{2}	100	3.2×10^{0}	2.5×10^{1}	5.4×10^{0}	2.6×10^{0}	1.5×10^{0}	1.3×10^{0}
1.0×10^{2}	250	1.4×10^{0}	6.0×10^{0}	1.8×10^{0}	8.9×10^{-1}	4.9×10^{-1}	4.5×10^{-1}
1.0×10^{2}	500	1.2×10^{0}	2.7×10^{0}	8.7×10^{-1}	4.8×10^{-1}	2.8×10^{-1}	2.6×10^{-1}
1.0×10^{2}	1000	1.1×10^{0}	1.5×10^{0}	5.0×10^{-1}	3.0×10^{-1}	1.9×10^{-1}	1.8×10^{-1}
1.0×10^{2}	3000	1.1×10^{0}	6.0×10^{-1}	2.4×10^{-1}	1.7×10^{-1}	1.2×10^{-1}	1.2×10^{-1}
1.0×10^{3}	50	1.7×10^{-1}	5.6×10^{-1}	2.1×10^{-1}	8.6×10^{-2}	5.7×10^{-2}	5.0×10^{-2}
1.0×10^{3}	100	4.7×10^{-2}	2.8×10^{-1}	6.6×10^{-2}	3.7×10^{-2}	2.7×10^{-2}	2.5×10^{-2}
1.0×10^{3}	250	2.3×10^{-2}	7.5×10^{-2}	2.8×10^{-2}	1.9×10^{-2}	1.6×10^{-2}	1.5×10^{-2}
1.0×10^{3}	500	2.0×10^{-2}	3.9×10^{-2}	1.9×10^{-2}	1.5×10^{-2}	1.3×10^{-2}	1.3×10^{-2}
1.0×10^{3}	1000	2.0×10^{-2}	2.5×10^{-2}	1.4×10^{-2}	1.3×10^{-2}	1.1×10^{-2}	1.1×10^{-2}
1.0×10^{3}	3000	1.9×10^{-2}	1.5×10^{-2}	1.1×10^{-2}	1.1×10^{-2}	9.9×10^{-3}	9.9×10^{-3}
1.0×10^{4}	50	4.7×10^{-3}	8.2×10^{-3}	3.5×10^{-3}	1.9×10^{-3}	1.7×10^{-3}	1.6×10^{-3}
1.0×10^{4}	100	1.9×10^{-3}	4.3×10^{-3}	1.7×10^{-3}	1.4×10^{-3}	1.3×10^{-3}	1.2×10^{-3}
1.0×10^{4}	250	1.2×10^{-3}	1.8×10^{-3}	1.2×10^{-3}	1.1×10^{-3}	1.1×10^{-3}	1.1×10^{-3}
1.0×10^{4}	500	1.0×10^{-3}	1.3×10^{-3}	1.1×10^{-3}	1.0×10^{-3}	1.0×10^{-3}	1.0×10^{-3}
1.0×10^{4}	1000	1.0×10^{-3}	1.1×10^{-3}	9.9×10^{-4}	9.7×10^{-4}	9.6×10^{-4}	9.6×10^{-4}
1.0×10^{4}	3000	1.0×10^{-3}	9.8×10^{-4}	9.4×10^{-4}	9.3×10^{-4}	9.2×10^{-4}	9.2×10^{-4}
1.0×10^{5}	50	3.5×10^{-4}	2.3×10^{-4}	1.5×10^{-4}	1.1×10^{-4}	1.1×10^{-4}	1.1×10^{-4}
1.0×10^{5}	100	1.6×10^{-4}	1.4×10^{-4}	1.1×10^{-4}	1.0×10^{-4}	1.0×10^{-4}	9.9×10^{-5}
1.0×10^{5}	250	1.0×10^{-4}	1.0×10^{-4}	9.6×10^{-5}	9.5×10^{-5}	9.5×10^{-5}	9.4×10^{-5}
1.0×10^{5}	500	9.5×10^{-5}	9.7×10^{-5}	9.3×10^{-5}	9.3×10^{-5}	9.3×10^{-5}	9.3×10^{-5}
1.0×10^{5}	1000	9.2×10^{-5}	9.3×10^{-5}	9.2×10^{-5}	9.2×10^{-5}	9.2×10^{-5}	9.2×10^{-5}
1.0×10^{5}	3000	9.1×10^{-5}	9.1×10^{-5}	9.1×10^{-5}	9.0×10^{-5}	9.0×10^{-5}	9.0×10^{-5}

TABLE III. The minimal exposures needed to make a 3σ discovery of WIMP annihilation in the Earth with the atmospheric background being vertical. The values given are for hard muon spectra and a muon energy threshold of 1 GeV.